NIH Public Access
Author Manuscript
J Magn Reson Imaging. Author manuscript; available in PMC 2012 December 1.

Published in final edited form as:
J Magn Reson Imaging. 2011 December ; 34(6): 1397–1404. doi:10.1002/jmri.22799.

Determination of Cranio-Spinal Canal Compliance Distribution by MRI: Methodology and Early Application in Idiopathic Intracranial Hypertension

Rong-Wen Tain, MS[1], **Ahmet M. Bagci, PhD**[1], **Byron L. Lam, MD**[3], **Evelyn M Sklar, MD**[1], **Birgit Ertl-Wagner, MD**[4], and **Noam Alperin, PhD**[1,2]

[1]Department of Radiology, University of Miami

[2]Department of Biomedical Engineering, University of Miami

[3]Bascom Palmer Eye Institute, University of Miami

[4]Department of Radiology, University of Munich, Germany

Abstract

PURPOSE—To develop a method for derivation of the cranial-spinal compliance distribution, assess its reliability, and apply to obese female patients with a diagnosis of Idiopathic Intracranial Hypertension (IIH).

MATERIALS AND METHODS—Phase contrast based measurements of blood and CSF flows to, from, and between the cranial and spinal canal compartments were used with lumped-parameter modeling to estimate systolic volume and pressure changes from which cranial and spinal compliance indices are obtained. The proposed MRI indices are analogous to pressure volume indices (PVI) currently being measured invasively with infusion based techniques. The consistency of the proposed method was assessed using MRI data from 7 aged healthy subjects. Measurement reproducibility was assessed using 5 repeated MR scans from one subject. The method was then applied to compare spinal canal compliance contribution in 7 IIH patients and 6 matched healthy controls.

RESULTS—In the healthy subjects, as expected, spinal canal contribution was consistently larger than the cranial contribution (average value of 69%). Measurement variability was 8%. In IIH, the spinal canal contribution is significantly smaller than normal controls (60 vs. 78%, $P<0.03$).

CONCLUSION—MRI based method for derivation of compliance indices analogous to PVI has been implemented and applied to healthy subjects. The application of the method to obese IIH patients points to the potential role of the spinal canal compartment in IIH.

Keywords

cranio-spinal compliance; CSF and blood flows; intracranial pressure; lumped parameter modeling; spinal canal compliance; phase contrast

INTRODUCTION

Mechanical compliance determines the ability of a compartment to accommodate a change in volume. A compliant compartment can accommodate a larger volume for a given change

Corresponding author: Noam Alperin, PhD, Physiologic Imaging and Modeling Laboratory, Department of Radiology and Biomedical Engineering, University of Miami, Miami, FL 33136, Tel: 305-243-8098, Fax: 305-243-3405, NAlperin@med.miami.edu.

NIH-PA Author Manuscript
NIH-PA Author Manuscript
NIH-PA Author Manuscript

NIH-PA Author Manuscript

NIH-PA Author Manuscript

NIH-PA Author Manuscript

in pressure. In vertebrates, the overall cranio-spinal compliance is determined by the sum of the individual compliances of the cranial and spinal canal compartments (1,2). Given that both compartments contribute to regulation of intracranial pressure (ICP), it is important to be able to determine how the overall cranio-spinal canal compliance is distributed to understand the role of the spinal canal compartment in ICP regulation, especially since the overall compliance changes with posture (3,4), with a change in ICP (2), and with different pathologies (5,6).

From anatomical consideration, it is expected that in the supine posture, when hydrostatic pressure is similar in the cranium and spinal canal, the spinal canal (SC) contribution to the total cranio-spinal (CS) compliance is larger than the cranial (CR) compartment contribution because the dura in the spinal canal, especially in the lumbar region and dural sac, is less confined by bony structures compared with the cranial vault. Over the last several decades different methods were proposed for estimation of the CS compliance (2,3,7–13). These methods rely on infusion of fluids into the cerebrospinal fluid (CSF) spaces and recording the change in CSF pressure under different infusion paradigms. Yet, infusion based approaches for estimation of the cranio-spinal compliance distribution provided disparate results (2,3,7,13).

Using a constant rate infusion method in dogs, Löfgren and Zwetnow found that the cranial contribution is smaller than the spinal canal contribution (7). Using a bolus injection method in cats, Marmarou *et al*. revealed a mono-exponential relationship between intracranial pressure and volume (2). The linear slope in a semi-logarithm scale of the derived pressure-volume curve was termed pressure-volume index (PVI). PVI is the factor by which pressure and elastance (e.g., inverse of compliance) are linearly related. In contrast to previous findings using the constant infusion method, they reported a larger compliance contribution from the cranial compartment, 68% vs. 32 % for the spinal canal. Fourteen years later, Magnaes applied the bolus method to estimate individual cranial and spinal compliances in patients with CSF blockage at the cervical level (3). They found that the cranial compartment contribution is smaller, about 37% of the total compliance. A third infusion method, a constant pressure infusion, applies a variable infusion rate to achieve several different constant pressure states (14). This approach utilizes the natural pressure pulsation to determine the PVI from the linear relationship between the amplitude of the pulsation and mean pressure (10). A constant pressure infusion test in conjunction with MRI measurements of blood and CSF flows to and between the cranio-spinal compartments was recently proposed by Wåhlin et al. to estimate the CS compliance distribution in supine aged healthy subjects, without the need to physically isolate the two compartments (13). In contrast to earlier report, that approach suggests a larger cranial contribution, 65%, vs. 35% from the spinal canal.

Following the work by Wåhlin et al. this paper proposes an entirely noninvasive approach to estimate the cranio-spinal compliance distribution by integrating a previously reported method for measurement of intracranial compliance (15) with a lumped-parameter modeling of the cranio-spinal system (16). The potential clinical relevance of this method is demonstrated by assessing the cranio-spinal compliance distribution in newly diagnosed obese female patients with Idiopathic Intracranial Hypertension (IIH). Cranio-spinal compliance distribution measurements were used to test the hypothesis that IIH in obese females is associated with reduced spinal canal compliance contribution due to increased abdominal pressure, which in turns, contributes to the elevated ICP.

NIH-PA Author Manuscript

NIH-PA Author Manuscript

NIH-PA Author Manuscript

MATERIALS AND METHODS

Materials and Data Acquisition

The study was approved by the IRB and all subjects provided informed consent. MR images were acquired from 3 different cohorts of subjects. Data from **7** aged healthy subjects (mean age 64 ±10 years) were used to test the consistency of the derivation of cranio-spinal compliance distribution. Elderly adults were studied to enable comparison with literature results (13). One healthy male subject (age 32) was scanned repeatedly 5 times to assess measurement reproducibility. Seven newly diagnosed female IIH patients (BMI of 33±5 kg/m^2, mean age of 28±10 years) and 6 healthy female subjects (BMI of 35±3 kg/m^2, mean age of 34±10 years) were studied to assess the role of cranio-spinal compliance distribution in IIH. The diagnosis of IIH was made based on modified Dandy criteria and confirmed by lumbar puncture (opening pressure ranged from 26 to 41 cmH2O). Presented symptoms include mild to severe headache, and mild to moderate papilledema (grading range was mostly 2 and 3).

MRI scans of the IIH and control subjects were performed using a 1.5T scanner and of the aged healthy subject using a 3T scanner (Siemens Medical Solution, Germany). The MRI brain protocol included anatomical imaging and two additional retrospectively gated velocity encoded cine phase contrast scans for quantitation of blood and CSF flows to and from the cranium (17). Blood flow was imaged using high velocity encoding (VENC) of 70 cm/sec. The CSF flow was imaged using a lower VENC of 7 cm/sec. Other imaging parameters include FOV of 14cm, slice thickness of 5–6 mm, acquisition matrix of 256×160, shortest repetition and echo times (43–52 ms and 7–10 ms), and flip angle of 20 degrees. Total arterial inflow to the cranium is derived by summation of flow through the internal carotid and vertebral arteries. Venous outflow is obtained by summation of the volumetric flow rates through the internal jugular veins, and through the three main secondary channels when present (e.g. epidural, vertebral, and deep cervical veins). Venous flow through the secondary channels is obtained from the low VENC images. Images were reconstructed into 32 cardiac phases using the same projected heart rate for both the blood and CSF flows.

Estimation of Cranio-Spinal Compliance using Pressure-Volume Indices

Estimation of the compliance is obtained from the PVI, which characterizes the compartment biomechanical property independently of the compliance state, as defined in Eq. [1] (2,18).

$$C = \frac{0.4343 \cdot PVI}{P} \quad [1]$$

where C and P are the compartment's compliance and pressure, respectively. The distribution of the compliance is then estimated by calculating the individual PVI of each sub-compartment using Eq. [2],

$$PVI = \frac{\Delta V}{\log_{10}\left(\frac{\Delta P}{P} + 1\right)} \quad [2]$$

where ΔV is the maximal volume change in the compartment, and ΔP and P are the pressure amplitude and mean pressure, respectively. The derivation of the PVI requires estimation of

NIH-PA Author Manuscript

NIH-PA Author Manuscript

NIH-PA Author Manuscript

the compartmental volume change (ΔV) and the relative pressure change ($\frac{\Delta P}{P}$). These parameters are obtained using the MRI measurements of volumetric arterial inflow and venous outflow to and from the cranium, and CSF flow between the cranium and the spinal canal (15). The associated pressure changes are derived using a previously reported lumped-parameter modeling (16).

MRI Measurements of the Compartmental Volume Change

The time-varying compartmental volume change waveforms are derived using the volumetric flow rates into and out of the specific compartment (15). A simplified diagram of the cranio-spinal compartment is shown (Fig. 1A). The inlet and outlet of the cranial compartment are the arterial inflow f_A, venous outflow f_V, and craniospinal CSF flow f_{CSF}. The spinal canal compartment has a single inlet and outlet for the CSF flow from and back to the cranium. The mathematical expressions of the volume changes of the cranio-spinal compartment and the two individual sub compartments are described in Eq. [3],

$$\Delta V_{CS}(i)=[f_A(i)-f_V(i)]\cdot\Delta t \quad [3A]$$

$$\Delta V_{CR}(i)=[f_A(i)-f_V(i)-f_{CSF}(i)]\cdot\Delta t \quad [3B]$$

$$\Delta V_{SC}(i)=f_{CSF}(i)\cdot\Delta t \quad [3C]$$

where i is the cardiac phase index sampled by time intervals of Δt. The maximal volume change of each compartment, which occurs in the systolic phase, is the peak to peak amplitude of volume change waveform. Eq. [4], which states that there is no change or accumulation of volume over the entire cardiac, is used to account for the small unmeasured venous outflow through secondary veins (15).

$$\sum_{\substack{cardiac\\cycle}} \Delta V_{CR}(i)=\sum_{\substack{cardiac\\cycle}} [f_A(i)-f_V(i)-f_{CSF}(i)]\cdot\Delta t=0 \quad (4)$$

Prediction of Pulsatile Pressure Dynamics using Lumped-Parameter Model

A previously described lumped-parameter model of the CSF flow dynamics in the cranio-spinal compartment (16), shown in Fig. 1B, is used to estimate the pulse pressure in each of the sub-compartments. The input of the model is the arterial minus venous blood flow and the output is the craniospinal CSF flow. The mechanical properties of cranial and spinal sub-compartments are lumped into flow resistances (R1 and R2) and compliances (C1 and C2), respectively. The inertia dominated CSF flow between cranio-spinal compartment (19) is modeled by an inductor, I2. The transfer function of the cranio-spinal system is shown in Eq. [5],

NIH-PA Author Manuscript

NIH-PA Author Manuscript

NIH-PA Author Manuscript

$$H(s)=\frac{F_{csf}(s)}{F_{av}(s)}=\frac{\frac{R1}{I2}s+\frac{1}{I2\cdot C1}}{s^2+\frac{1}{I2}(R1+R2)s+\frac{1}{I2}(\frac{1}{C1}+\frac{1}{C2})} \quad (5)$$

where H(s) is the frequency response of the transfer function in the Laplace domain. The reliability of the modeled system dynamics is assessed by the degree of similarity between the measured and the model predicted CSF flow waveforms using percentage of fit (1-normalized Euclidean distance of error) defined in Eq. [6].

$$fit(\%)=(1-\frac{|\boldsymbol{f}_{mea}-\boldsymbol{f}_{sim}|}{|\boldsymbol{f}_{mea}-mean(\boldsymbol{f}_{mea})|})\times 100\% \quad (6)$$

The pressure pulsation (ΔP) in each of the sub-compartments is then derived based on compliance-flow relationship shown in Eq. [7],

$$\Delta P(i)=\frac{1}{C_x}f_x(i)\cdot\Delta t \quad (7)$$

where f_x and C_x are the net volumetric flow rate and compliance of each sub-compartment, respectively. While the model enables the derivation of the pressure change it does not provide an absolute mean pressure (P). However, since subjects are scanned in the supine posture, the mean pressure in each of the sub-compartment is assumed to be the same. This assumption was previously confirmed using invasive pressure measurement (20). The cranio-spinal compliance distribution is then obtained from the ratio of the individual PVI of each sub-compartment.

Estimation of Compliance Distribution from Subject Specific Transfer Function

An estimate of compliance distribution can also be derived from the lumped-parameter model. Therefore the consistency of the PVI derived compliance distribution is assessed by comparing the PVI based results with an estimate obtained using the subject-specific transfer function that is derived from MR based measurements of cerebral blood and CSF flows (Eq. [5]). While the transfer function does not provide absolute compliance values, the compliance distribution is available through the coefficients shown as Eq. [8].

$$SCCC(\%)=\frac{C2}{C1+C2}=\frac{\frac{1}{I2\cdot C1}}{\frac{1}{I2}(\frac{1}{C1}+\frac{1}{C2})}\times 100\% \quad (8)$$

Reliability of Compliance Distribution Measurements

The reliability of the derived compliance distribution is assessed by testing the consistency and reproducibility of the results. Consistency is assessed by comparing the distribution ratio calculated directly from the transfer function based on Eq. [8] with the PVI derived distribution as well as by comparing two simulated conditions, “communicating” and “isolated” cranio-spinal sub-compartments, which simulates the invasive approach for derivation of the compliance distribution. The isolation of the compartment enables estimation of its contribution to the overall compliance independently of the other

NIH-PA Author Manuscript

NIH-PA Author Manuscript

NIH-PA Author Manuscript

compartment. Compartments isolation was achieved by increasing R1 or R2 values until the maximal volume change in the "isolated" compartment is less than 0.05 ml. Reliability is concluded if similar compliance distributions are obtained for the isolated and communicating states, and if the PVI based values are in agreement with values derived from the transfer function. Measurement reproducibility is determined from 5 repeated MR scans on the same subject.

Compliance Distribution in Idiopathic Intracranial Hypertension

The new measurement of compliance distribution was assessed in the cohorts of IIH patients and healthy controls to test the hypothesis that IIH in obese females of childbearing age is associated with reduced spinal canal compliance buffering. An unpaired sample t-test was used to determine the statistical significance of the differences. A P value below 0.05 was considered significant.

RESULTS

An example of velocity encoded images of blood and CSF flows and the calculated arterial, venous, arterial minus venous and CSF volumetric flow rate waveforms is shown (Fig. 2). The CSF flow waveform is plotted together with the arterial minus venous waveforms in Fig 2d, to demonstrate the input/output relationship of these two waveforms. An example of model-derived CSF flow waveform together with the measured waveform is shown (Fig. 3). The degree of similarity between the measured and the modeled waveform for this example is 86%. An overall high degree of similarity was obtained between the modeled and measured waveforms. The mean and SD of *fit*(%) for the 25 MRI scans from 21 subjects were 78±7%.

The mean value of the computed contribution of the spinal canal to the overall cranio-spinal compliance obtained using the transfer functions for the 7 aged healthy subjects is 69±16%. This value is consistent with values derived using the PVI calculation for the communicating state, 68±13%, (Table 1A), and the isolated state 66±13% (Table 1B).

In contrast to the similar PVI values obtained for the "communicating" and the "isolated" states, the maximal volume change are different between the two states as expected (Table 1). In the communicating state, the average maximal volume change in the cranial and spinal sub-compartments are 0.81 and 0.86 mL, respectively. Yet, a smaller pulse pressure is obtained in the spinal canal, the sub-compartment with the larger compliance, as expected for a compartment with the larger compliance (Table 1A). Similar behavior is seen in the "isolated" state, except that the respective volume changes, 1.51 and 1.47 mL, as well as the resulting pulse pressure, 2.41 and 1.44 mmHg, are much larger. Again, this is expected, because only one sub-compartment at a time is "functioning" to accommodate the pulsatile volumetric blood flow.

The compliance distribution measurement variability estimated by the relative SD of the repeated MR scans in the same individual is 8%. The mean and SD values of the 5 repeated measurements of spinal canal compliance contribution are 74±6 %. The measurement variability of total cerebral blood flow in the same individual is 7% (818±56 ml/min).

The application of the compliance distribution measurement to IIH yields a statistically significant reduced spinal canal compliance contribution in the newly diagnosed IIH patients compared with the healthy subject ($P<0.03$). The mean spinal canal compliance contribution from the in IIH patients and the healthy subjects are 60±14% and 78±12%, respectively.

NIH-PA Author Manuscript

NIH-PA Author Manuscript

NIH-PA Author Manuscript

DISCUSSION

Previously reported invasive measurements of the cranio-spinal compliance distribution provide conflicting observations regarding the contribution of the spinal canal to the overall cranio-spinal compliance. From anatomical consideration, it is expected that the spinal canal contribution is larger than the cranial contribution due to the dura being less confined by the bony structures, especially in the lumbar region, and because CSF can expand into the dural sleeve of the nerve root (21). MRI provides a noninvasive means to estimate volumetric flow rates into and out of the cranio-spinal system and its individual sub compartments (6,22). This capability was employed in the current study in combination with lumped-parameter modeling (16) to noninvasively estimate the cranio-spinal compliance distribution. The reliability of this approach is demonstrated by the consistency of the compliance distribution values obtained using the subject-specific transfer function and direct estimation based on the ratio of the volume change and pulse pressure during the cardiac cycle. The obtained values of the spinal canal contribution are 69 and 68%, respectively. In addition, similar spinal canal compliance contributions are obtained when the contribution is estimated under a simulated isolated state, 66%, which is analogous for the invasive approach for quantitation of the compliance distribution. The similar value supports the consistency of the derivation and the validity of the approach. All the 3 approaches yield a larger spinal canal compliance contribution compared to the cranial sub-compartment, as expected from anatomical consideration. The derived value of about 2:1 (SC:CR) compliance distribution is in good agreement with previous observation of spinal canal contribution of 63% in humans (3).

The robustness of the compliance distribution measurement is further supported by the small measurement variability of about 8% as demonstrated in 5 repeated MRI scans. The spinal compliance contribution measurement variability is on the same order of the tCBF measurement variability of 7% found in the same subject. It is likely that the normal physiological variability in the volumetric blood flow rates is the primary contribution to the variability in the measurement of the spinal canal compliance contribution. The tCBF measurement variability found in this study is in agreement with a previously reported variability of 7.1% derived from three repeated MR scans of 15 healthy subjects (23).

In contrast to our results, Wåhlin *et al* found that the cranial compliance is larger than the spinal canal compliance, 65% vs 35%, resepcitvely (13). Their novel approached combined for the first time MRI flow measurements with invasive infusion measurements to derive the relative compliance contribution of each compartment. CSF and blood flows were used to obtained volumetric changes and the invasive constant pressure infusion method was used to estimate the ratio of pulse pressure and mean pressure. Our work expands on Wåhlin's work with two major differences; first, actual venous outflow is used to calculate the volume change while their approach assumed a constant venous outflow. The second difference is the utilization of the lumped-parameter modeling in conjunction with the MRI flow measurements to estimate the pulse pressure magnitude in each compartment, instead of the infusion test. To demonstrate that indeed these differences account for the contradicting findings regarding maximal volume change in each of the sub compartment were calculated for the 7 healthy elderly subjects twice, once using the actual venous outflow and once using a constant, non-pulsatile venous outflow. Differences in the calculated volume change due to the venous outflow contribution obtain in one of these subjects are demonstrated in Fig. 4. The volume change during the cardiac cycle in each of the sub-compartment and the global cranio-spinal volume change are shown for an actual venous outflow and for an assumed constant venous outflow. The average maximal volume change values from the 7 subjects are summarized in Table 2. The venous outflow affects the derivation of the volume change in the cranial sub-compartment and therefore of the overall cranio-spinal compartment

NIH-PA Author Manuscript

NIH-PA Author Manuscript

NIH-PA Author Manuscript

(Table 2). With constant venous flow, the average maximal volume change in the cranial compartment is larger by 51%. A larger volume change implies a larger compliance, thus the overestimating of the cranial compliance. The volume change in the spinal canal compartment is unaffected by the cerebral venous outflow.

This observation is further validated by the derivation of the average spinal canal compliance using constant and actual venous outflow in our cohorts. The results which are summarized in Table 3 demonstrate that the average value of the spinal canal compliance contribution increases from 40% to 49% when actual venous outflow is accounted for. This value is still smaller than the value of 69% obtained using our method. A second factor that contributed to the overestimation of the cranial compliance is assumed similar pulse pressure amplitude in both the cranial and the spinal canal sub-compartments. The invasive method used by Wåhlin *et al* measures the pulse pressure in the spinal canal and the same value is assumed in the cranium. This assumption contrasts reports documenting higher pulse pressure in the cranium (24,25). The lumped-parameter model used in our approach allows to estimation of the pulse pressure in each compartment individually.

A potential clinical relevance for determining cranio-spinal compliance distribution is demonstrated in the application of the method toward elucidating the pathophysiology of neurological disorders associated with altered ICP. IIH is associated with periods of considerably elevated CSF pressure and it is commonly occurring in obese females (26). A statistically significant smaller spinal canal compliance contribution was found in our homogenous cohort of IIH patients compared with healthy female of similar age and BMI, 60±14% vs. 78±12%, respectively.

Reduced compliance in the spinal compartment, which normally provides the majority of the cranio-spinal compliance, is therefore a likely contributor for the increased ICP in IIH. IIH is believed to be associated with impaired CSF absorption (27). Impaired absorption is likely to increase CSF volume, which in conjunction with reduced compliance buffering would result in elevated ICP. The association between IIH and obesity further support the involvement of the spinal canal compartment in IIH. MR imaging of the spinal CSF spaces demonstrated that obesity is associated with reduced CSF cross-sectional area explained by inward displacement of the foramen contents caused by increased abdominal pressure (21). Lee et al further demonstrates that lumbar CSF volume can be reduced by increasing abdominal pressure (28). These observations point to a potential mechanism that causes reduced spinal canal compliance in IIH, i.e., an increased abdominal pressure limits the expansion of the spinal canal CSF spaces.

Lumped-parameter modeling has been previously applied to describe CSF dynamics and has contributed considerably to our current understanding of the cranio-spinal system (18,29). These models focused on the CSF circulation by formulating the relationship between CSF formation, absorption, compliance and pressure. The modeling used in our work focuses on the pulsatile aspect of the CSF dynamics assessing the craniospinal compliance distribution from the relationships between CSF and blood flows in the individual compartments. This model enables the utilization of established invasive infusion based methodologies toward noninvasive estimation of the CS biomechanical characteristics through the determination of the CS compliance distribution.

A limitation of the proposed approach is related to the fact that direct arterial inflow and venous outflow to and from the spinal canal compartment through the spinal arteries and veins are not measured and accounted for in the calculation of the volume change in the spinal canal. However, we estimate that the volumetric changes due to the blood component would be considerably smaller than the volume change due to the cranio-spinal CSF flow.

NIH-PA Author Manuscript

NIH-PA Author Manuscript

NIH-PA Author Manuscript

The total volumetric arterial flow to the spinal cord is considerably smaller than the total cerebral volumetric blood flow as the spinal cord tissue volume is about 30 times smaller than the brain (30,31). In addition, the smaller volumetric flow is relatively less pulsatile than the blood flow through the internal carotid and vertebral arteries. Thereby the contribution from the trans-spinal canal net blood flow is expected to be small and from practical constrain could be neglected.

In summary, an MRI based method that combines measurements of blood and CSF volumetric flows to and from the cranio-spinal system and lumped-parameter modeling is proposed for noninvasive estimation of the cranio-spinal compliance contribution. The method yields a larger compliance contribution from the spinal compartment than the cranial compartment in healthy subjects consistent with anatomical consideration. The application of the method to overweight and obese female IIH patients revealed a significantly smaller SC compliance contribution compared to healthy controls. The smaller spinal compliance buffering most likely limits its capacity to accommodate an increase in CSF volume, which in turn, contributes to the increased ICP in IIH.

Acknowledgments

Grant Support: Supported by the National Institute of Neurological Disorders and Stroke R01 NS052122 NA.

References

1. Löfgren J, von Essen C, Zwetnow N. The pressure-volume curve of the cerebrospinal fluid space in dogs. Acta Neurol Scand. 1973; 49:557–574. [PubMed: 4770652]
2. Marmarou A, Shulman K, LaMorgese J. Compartmental analysis of compliance and outflow resistance of the cerebrospinal fluid system. J Neurosurg. 1975; 43:523–534. [PubMed: 1181384]
3. Magnaes B. Clinical studies of cranial and spinal compliance and the craniospinal flow of cerebrospinal fluid. Br J Neurosurg. 1989; 3:659–668. [PubMed: 2627285]
4. Alperin N, Lee S, Sivaramakrishnan A, Hushek S. Quantifying the effect of posture on intracranial physiology in humans by MRI flow studies. J Magn Reson Imaging. 2005; 22:591–596. [PubMed: 16217773]
5. Maset AL, Marmarou A, Ward JD, et al. Pressure-volume index in head injury. J Neurosurg. 1987; 67:832–840. [PubMed: 3681422]
6. Miyati T, Mase M, Kasai H, et al. Noninvasive MRI assessment of intracranial compliance in idiopathic normal pressure hydrocephalus. J Magn Reson Imaging. 2007; 26:274–278. [PubMed: 17610284]
7. Löfgren J, Zwetnow N. Cranial and spinal components of the cerebrospinal fluid pressure-volume curve. Acta Neurol Scand. 1973; 49:575–585. [PubMed: 4770653]
8. Mann J, Butler A, Rosenthal J, Maffeo C, Johnson R, Bass N. Regulation of intracranial pressure in rat, dog, and man. Ann Neurol. 1978; 3:156–165. [PubMed: 655666]
9. Shapiro K, Marmarou A, Shulman K. Characterization of clinical CSF dynamics and neural axis compliance using the pressure-volume index: I. The normal pressure-volume index. Ann Neurol. 1980; 7:508–514. [PubMed: 7436357]
10. Avezaat C, van Eijndhoven J. Clinical observations on the relationship between cerebrospinal fluid pulse pressure and intracranial pressure. Acta Neurochir (Wien). 1986; 79:13–29. [PubMed: 3953320]
11. Czosnyka M, Batorski L, Laniewski P, Maksymowicz W, Koszewski W, Zaworski W. A computer system for the identification of the cerebrospinal compensatory model. Acta Neurochir (Wien). 1990; 105:112–116. [PubMed: 2275420]
12. Raabe A, Czosnyka M, Piper I, Seifert V. Monitoring of intracranial compliance: correction for a change in body position. Acta Neurochir (Wien). 1999; 141:31–36. discussion 35–36. [PubMed: 10071684]

NIH-PA Author Manuscript

NIH-PA Author Manuscript

NIH-PA Author Manuscript

13. Wåhlin A, Ambarki K, Birgander R, Alperin N, Malm J, Eklund A. Assessment of craniospinal pressure-volume indices. AJNR Am J Neuroradiol. 2010; 31:1645–1650. [PubMed: 20595369]
14. Ekstedt J. CSF hydrodynamic studies in man. 1. Method of constant pressure CSF infusion. J Neurol Neurosurg Psychiatry. 1977; 40:105–119. [PubMed: 864474]
15. Alperin N, Lee S, Loth F, Raksin P, Lichtor T. MR-Intracranial pressure (ICP): a method to measure intracranial elastance and pressure noninvasively by means of MR imaging: baboon and human study. Radiology. 2000; 217:877–885. [PubMed: 11110957]
16. Tain R, Alperin N. Noninvasive intracranial compliance from MRI-based measurements of transcranial blood and CSF flows: indirect versus direct approach. IEEE Trans Biomed Eng. 2009; 56:544–551. [PubMed: 19389680]
17. Tain R, Ertl-Wagner B, Alperin N. Influence of the compliance of the neck arteries and veins on the measurement of intracranial volume change by phase-contrast MRI. J Magn Reson Imaging. 2009; 30:878–883. [PubMed: 19787740]
18. Marmarou A, Shulman K, Rosende R. A nonlinear analysis of the cerebrospinal fluid system and intracranial pressure dynamics. J Neurosurg. 1978; 48:332–344. [PubMed: 632857]
19. Loth F, Yardimci M, Alperin N. Hydrodynamic modeling of cerebrospinal fluid motion within the spinal cavity. J Biomech Eng. 2001; 123:71–79. [PubMed: 11277305]
20. Lenfeldt N, Koskinen L, Bergenheim A, Malm J, Eklund A. CSF pressure assessed by lumbar puncture agrees with intracranial pressure. Neurology. 2007; 68:155–158. [PubMed: 17210899]
21. Hogan Q, Prost R, Kulier A, Taylor M, Liu S, Mark L. Magnetic resonance imaging of cerebrospinal fluid volume and the influence of body habitus and abdominal pressure. Anesthesiology. 1996; 84:1341–1349. [PubMed: 8669675]
22. Alperin N, Mazda M, Lichtor T, Lee SH. From Cerebrospinal Fluid Pulsation to Noninvasive Intracranial Compliance and Pressure Measured by MRI Flow Studies. CURRENT MEDICAL IMAGING REVIEWS. 2006; 2:117–130.
23. Spilt A, Box FM, van der Geest RJ, et al. Reproducibility of total cerebral blood flow measurements using phase contrast magnetic resonance imaging. J Magn Reson Imaging. 2002; 16:1–5. [PubMed: 12112496]
24. Lindgren S, Rinder L. Production and distribution of intracranial and intraspinal pressure changes at sudden extradural fluid volume input in rabbits. Acta Physiol Scand. 1969; 76:340–351. [PubMed: 5823865]
25. Eide P, Brean A. Lumbar cerebrospinal fluid pressure waves versus intracranial pressure waves in idiopathic normal pressure hydrocephalus. Br J Neurosurg. 2006; 20:407–414. [PubMed: 17439094]
26. Dhungana S, Sharrack B, Woodroofe N. Idiopathic intracranial hypertension. Acta Neurol Scand. 2010; 121:71–82. [PubMed: 19930211]
27. Karahalios DG, Rekate HL, Khayata MH, Apostolides PJ. Elevated intracranial venous pressure as a universal mechanism in pseudotumor cerebri of varying etiologies. Neurology. 1996; 46:198–202. [PubMed: 8559374]
28. Lee R, Abraham R, Quinn C. Dynamic physiologic changes in lumbar CSF volume quantitatively measured by three-dimensional fast spin-echo MRI. Spine (Phila Pa 1976). 2001; 26:1172–1178. [PubMed: 11413433]
29. Stevens SA, Stimpson J, Lakin WD, Thakore NJ, Penar PL. A model for idiopathic intracranial hypertension and associated pathological ICP wave-forms. IEEE Trans Biomed Eng. 2008; 55:388–398. [PubMed: 18269974]
30. Ko H, Park J, Shin Y, Baek S. Gross quantitative measurements of spinal cord segments in human. Spinal Cord. 2004; 42:35–40. [PubMed: 14713942]
31. Steen R, Hamer R, Lieberman J. Measuring brain volume by MR imaging: impact of measurement precision and natural variation on sample size requirements. AJNR Am J Neuroradiol. 2007; 28:1119–1125. [PubMed: 17569971]

NIH-PA Author Manuscript

NIH-PA Author Manuscript

NIH-PA Author Manuscript

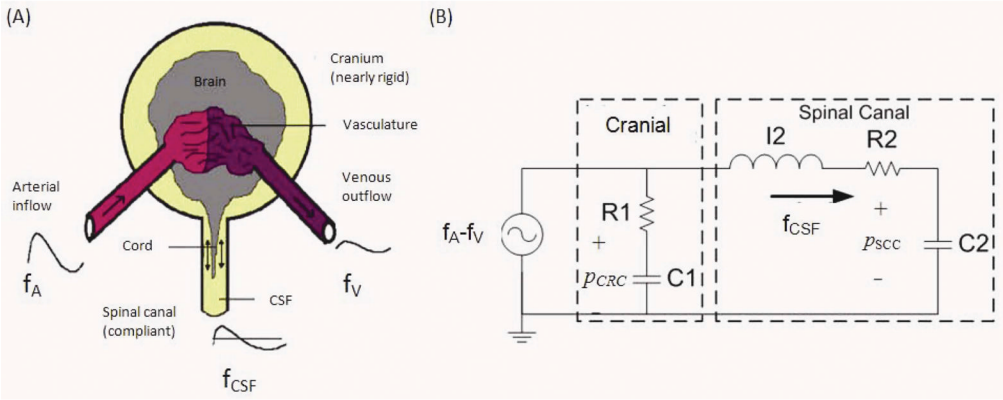

FIG. 1.

(A) The schematic diagram of compartmental cranio-spinal system. (B) Electrical circuit analogy of the flow dynamics in the cranio-spinal sub-compartments. R1, R2, C1 and C2 are the resistances to flow and compliances of the cranial and spinal sub-compartments, respectively. I2 represents the inertia component of the CSF flow (f_{CSF}) to and from the spinal canal. The driving force for the flow dynamics is the net blood flow ($f_A - f_V$) to the cranio-spinal system.

NIH-PA Author Manuscript
NIH-PA Author Manuscript
NIH-PA Author Manuscript

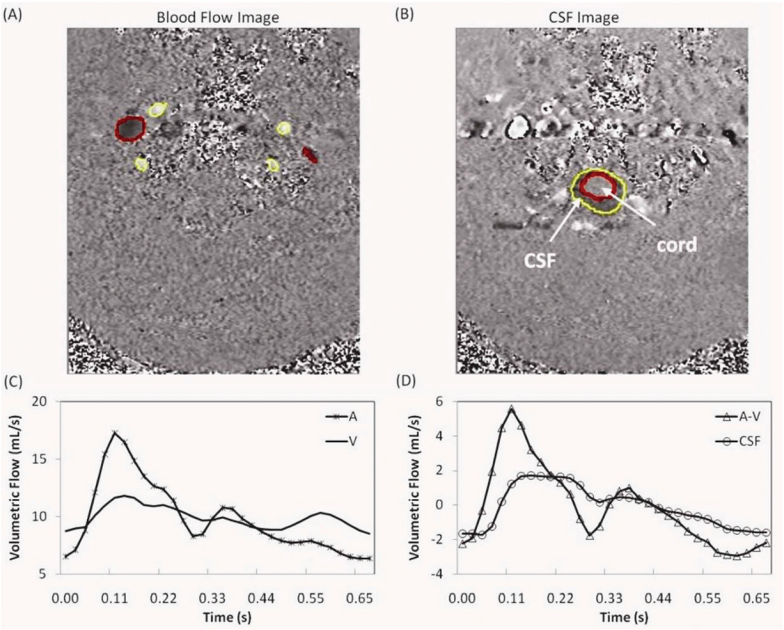

FIG. 2.

An example of velocity encoded MRI images of blood flow (image A) and CSF flow (image B) used for derivation of the blood and CSF volumetric flow rate waveforms (images C and D, respectively). Flow in the cranial direction shown in white pixels and in caudal direction is dark. The lumen boundaries of the arteries and CSF space are shown in black and the boundaries of the internal jugular veins lumens are shown in white. The arterial, venous and CSF volumetric flow waveforms over one cardiac cycle are marked by A, V, and CSF, respectively. The net transcranial blood flow (arterial minus venous flow) is marked by A–V (images D).

NIH-PA Author Manuscript

NIH-PA Author Manuscript

NIH-PA Author Manuscript

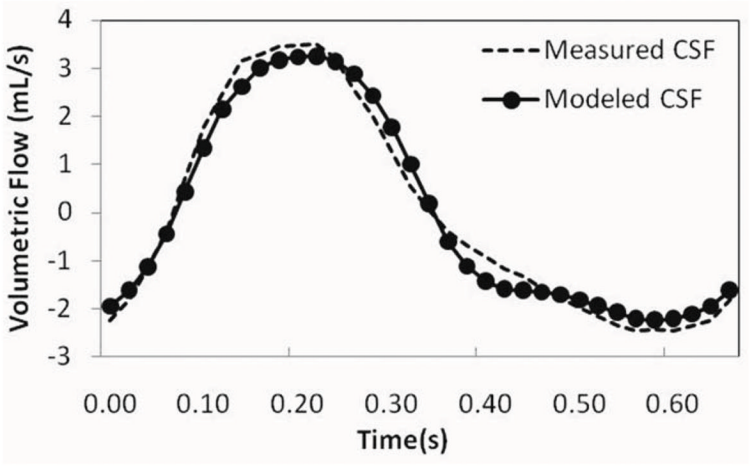

FIG. 3.

Plot of the measured CSF (−) and the modeled CSF (●) flow waveforms derived from one of the subjects. The similarity between two waveforms is 86% (fit%).

NIH-PA Author Manuscript

NIH-PA Author Manuscript

NIH-PA Author Manuscript

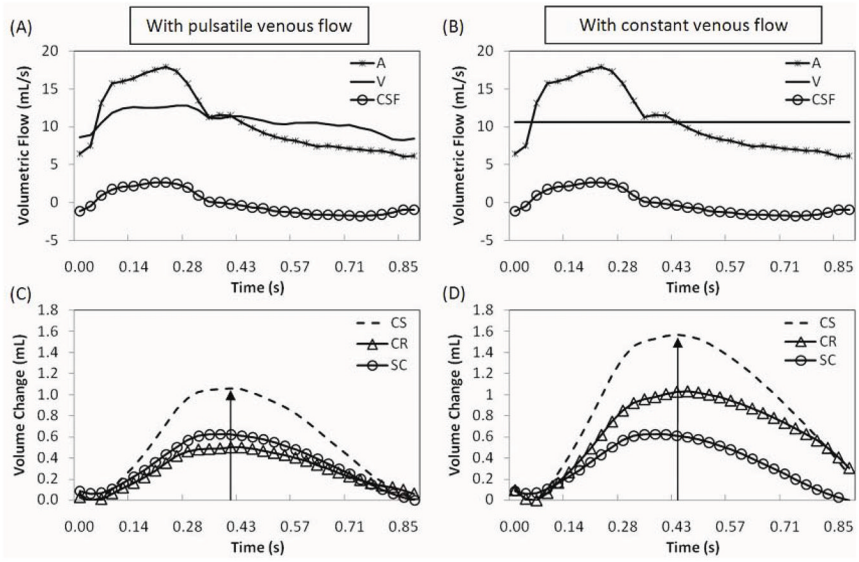

FIG. 4.

The influence of venous flow dynamics on the derivation of the volume change waveforms. Examples of arterial, venous, and CSF flow waveforms from one of the subjects used for derivation of the volume change waveforms are shown in A. Actual venous outflow is replaced with constant venous outflow in B. Corresponding cranio-spinal, cranial and spinal compartmental volume change waveforms are shown in C and D. A larger peak-to-peak volume change is observed in the cranial compartment when a non-pulsatile venous dynamics is used (D).

NIH-PA Author Manuscript

NIH-PA Author Manuscript

NIH-PA Author Manuscript

Table 1

Compliance distribution using PVI calculation under two conditions: (A) communicating compartments and (B) isolated compartments.

(A)

	CR	SC	$\frac{SC}{CR+SC}(\%)$
PVI_{comm} (ml)	11.69±3.30	34.43±28.23	68±13%
ΔV (ml)	0.81±0.24	0.86±0.29	-
ΔP (mmHg)	1.29±0.34	0.79±0.59	-

(B)

	CR	SC	$\frac{SC}{CR+SC}(\%)$
PVI_{iso} (ml)	12.74±3.31	32.94±24.54	66±13%
ΔV (ml)	1.51±0.45	1.47±0.42	-
ΔP (mmHg)	2.41±0.84	1.44±1.12	-

NIH-PA Author Manuscript

NIH-PA Author Manuscript

NIH-PA Author Manuscript

Table 2

Compartmental volume change (ΔV) obtained with pulsatile and constant venous outflow.

	ΔV (mL)		
Compartment	**With pulsatile venous flow**	**With constant venous flow**	**Difference (%)**
CS	1.16±0.41	1.54±0.48	37±27%
CR	0.66±0.19	0.98±0.28	51±39%
SC	0.67±0.33	0.67±0.33	-

NIH-PA Author Manuscript

NIH-PA Author Manuscript

NIH-PA Author Manuscript

Table 3

Compartmental PVI derived using a constant and pulsatile venous outflow.

	CS	CR	SC	$\frac{SC}{CR+SC}(\%)$
PVI_C (ml)	7.36±2.28	4.42±1.38	2.94±1.05	40±6%
PVI_P (ml)	5.48±1.95	2.97±0.94	2.94±1.05	49±7%

C - Constant venous outflow

P - Pulsatile venous outflow